ACS APPLIED MATERIALS & INTERFACES

Research Article

Cite This: ACS Appl. Mater. Interfaces 2019, 11, 31427−31433

www.acsami.org

A Novel Electrochemiluminescent Immunoassay Based on Target Transformation Assisted with Catalyzed Hairpin Assembly Amplification for the Ultrasensitive Bioassay

Hu-Xin Lei,[†,§] Chang-Chun Niu,[†,§] Tian Li,[†] Ya-Fang Wan,[†] Wen-Bin Liang,[‡] Ruo Yuan,[‡] and Pu Liao*[,†]

[†]Department of Laboratory Medicine, Chongqing General Hospital, Chongqing 400014, China

[‡]Key Laboratory of Luminescent and Real-Time Analytical Chemistry (Southwest University), Ministry of Education, College of Chemistry and Chemical Engineering, Southwest University, Chongqing 400715, People's Republic of China

Supporting Information

ABSTRACT: In this work, we constructed a novel electrochemiluminescent (ECL) strategy based on sandwich immunoassay-induced target transformation assisted with catalyzed hairpin assembly (CHA) amplification for ultrasensitive bioassay with cysteine-rich protein 61 (CCN1) as a model. First, the target CCN1 could be equally transformed into the specific oligonucleotide (initiator I) labeled on the detection antibody based on the specific sandwich immunoassay. In addition, the initiator I triggered an efficient nonenzymatic CHA amplification in the presence of ferrocene-labeled hairpin 1 (Fc-H1) and hairpin 2 (H2) to produce massive hybrids (Fc-H1−H2) containing a sticky end labeled with ferrocene. Finally, Fc-H1−H2 could be immobilized on the capture probe single-stranded DNA (ssDNA)-modified electrode through the hybridization between the sticky end of Fc-H1−H2 and ssDNA, and a significantly quenched ECL signal could be obtained due to the efficient quench effect between ferrocene and the ECL indicator, ruthenium(II) tris(4,4′-dicarboxylicacid-2,2′-bipyridyl) [$Ru(dcbpy)_3^{2+}$], immobilized on the surface of the electrode, which was related to the concentration of target CCN1. As expected, the proposed ECL biosensor exhibited a relatively low detection limit of 3.9 fg/mL in a linear range from 10 fg/mL to 100 ng/mL. This ECL strategy inspired the clinical examination of the biomarker CCN1, providing potential application in early diagnosis and malignant monitoring of cancer.

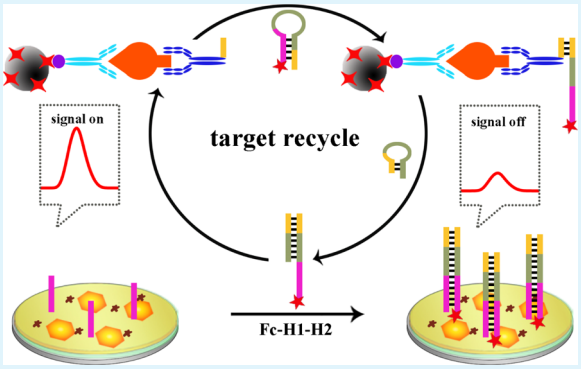

KEYWORDS: *electrochemiluminescent biosensor, sandwich immunoassay, target transform, early cancer diagnosis, CCN1, catalyzed hairpin assembly*

1. INTRODUCTION

Nowadays, cancer is still the greatest threat to human health all around the world with high prevalence and mortality.[1,2] Along with the significant improvements for treatments on cancer, it has been reported that cancer is not horrible and some cancers could be partly treated, but just some individual cases in the early stages without metastasis,[3,4] although, unfortunately, its prevalence and mortality are still far from decreasing because most patients usually were initially diagnosed with cancers in the middle or late stages even with malignant metastasis,[5] challenging with suitable biomarkers, efficient strategies, and sensitive assays to early diagnosis.[6,7] Cysteine-rich protein 61 (CCN1, a secreted matricellular protein), as the most important member of the CCN family proteins, plays a pivotal role in many cancers, such as acute myeloid leukemia,[8] breast cancer,[9] colorectal cancer,[10] osteosarcoma,[11] glioblastoma,[12] and so on. Previous references have confirmed that the overexpression of CCN1 could induce the disorder behaviors of a particular signaling pathway resulting in cell migration and cellular survival,[13,14] suggesting that CCN1 could be used as an efficient biomarker for screening, diagnosis, and prognosis of malignant cancers.[15,16] Currently, CCN1 was normally detected by an immunohistochemical analysis[17] and enzyme-linked immunosorbent assay (ELISA).[18] These methods were far from the early diagnosis of cancers via the sensitive detection of CCN1 because of the limitation of the high background signal and low sensitive determination. Thus, it is urgent to construct an accurate and rapid method to access the sensitive detection of CCN1 for the early diagnosis of cancers.

Recently, electrochemiluminescent (ECL) technology has been employed as one of the potential strategies for biomarker protein detection due to its excellent characteristics of a low-background signal, high sensitivity and specificity, simple operation, and rapid response, which not only received

Received: July 16, 2019
Accepted: July 31, 2019
Published: July 31, 2019

DOI: 10.1021/acsami.9b12428
ACS Appl. Mater. Interfaces 2019, 11, 31427−31433

Scheme 1. Schematic Illustration of the Sandwich-Based Target Transformation, CHA Amplification Process (A), and ECL Biosensor Preparation for CCN1 Detection (B)

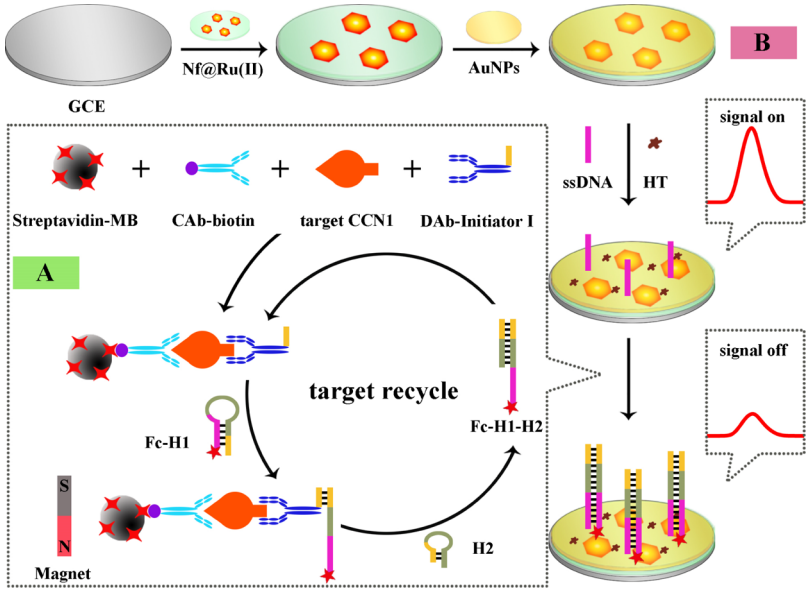

comparatively satisfied achievements, but also provided a promising research direction for the detection of biomarkers.[19−21] For example, Wang's group reported a label-free ECL biosensor on the basis of molybdenum carbides as the nanocarriers to immobilize luminol-capped Au nanoparticles as an efficient ECL reagent for the sensitive determination of α-fetoprotein (AFP) regarded as a core hepatocellular carcinoma biomarker with sixfold higher sensitivity and significantly improved ECL performances.[22] In spite of the advantages in these ECL strategies just by improving the immobilization of ECL luminescent reagents or co-reactants, they were still far from the ultrasensitive determination of CCN1 for early diagnosis of cancers. As well-known, protein could not be amplified by itself in the detection process.[23] On the contrary, it is possible to implement the amplification strategy for protein detection via a sandwich immunoassay by modifying the nucleotide sequence onto the secondary antibody and introducing nucleic acid amplification technique.[24,25] A catalyzed hairpin assembly (CHA) has been considered to be an extraordinarily versatile tool to construct an efficient nonenzymatic signal amplification with rapid response and low background for protein analysis.[26,27] Therefore, effectively applying CHA technology in an ECL biosensor could not only simplify the operation process, but also expect significantly improved detection performances, especially sensitivity.

Briefly, a novel ECL strategy was proposed based on sandwich immunoassay-induced target transformation with CHA amplification for the ultrasensitive detection of CCN1. As is shown in Scheme 1B, the ruthenium(II) tris(4,4′-dicarboxylicacid-2,2′-bipyridyl) [$Ru(dcbpy)_3^{2+}$] as an ECL luminophore was immobilized on the glass carbon electrode (GCE) surface with the assistant of efficient Nafion mediate modification. In addition, gold nanoparticles (AuNPs) with good electron transfer and larger surface area was electrochemically deposited on the electrode surface to immobilize the capture probe, single-stranded DNA (ssDNA) labeled with −SH. After that, hexanethiol (HT) was used to block the nonspecific recognition sites. At the same time, the manufacturing process of the dual antibody sandwich complex and CHA amplification were described in Scheme 1A. Primarily, NHS-biotin and the oligonucleotide initiator I were labeled onto the capture antibody (CAb) and the detection antibody (DAb) as CAb-biotin and DAb-initiator I, respectively. Subsequently, the streptavidin-magnetic beads were employed as the recycle carrier to immobilize a lot of CAb-biotin via specific biotin−streptavidin recognition. In the presence of target CCN1, CAb-biotin−streptavidin magnetic beads could immediately capture CCN1 and bind with DAb-initiator I to realize the effective transformation from target CCN1 to initiator I. Immediately, initiator I on DAb opened the hairpin structure of ferrocene-labeled H1 and generated a new toehold that could bind the overhang of the hairpin structure of H2. Based on these reactions, the initiator I could be released for the further hybrid amplification, resulting in the massive assembly of a double-stranded structure Fc-H1−H2 duplex with the sticky end labeled with ferrocene. Eventually, the Fc-H1−H2 duplex could be located on the surface of the electrode based on the specific hybridization between the sticky end of Fc-H1−H2 and ssDNA on the electrode surface, performing a dramatically decreasing signal due to the efficient quench effect of ferrocene on the ECL indicator, $Ru(dcbpy)_3^{2+}$. Thus, the concentration of target CCN1 could be quantitatively detected via the change of the ferrocene-related decreasing ECL signal. The proposed ECL strategy of combining the highly specific immune recognition of the sandwich assay with the efficient signal amplification technique of CHA realized the ultrasensitive determination of CCN1 for the first time, which demonstrated a promising application in early diagnosis and prognosis assessment of cancers.

2. EXPERIMENTAL SECTION

2.1. Materials and Reagents. Streptavidin-coated magnetic beads, HT (96%), tripropylamine (TPrA), Nafion (5%), and gold chloride tetrahydrate ($HAuCl_4 \cdot 4H_2O$) were received from Sigma Chemical Co. (St. Louis, MO, USA). CCN1 fusion protein and CCN1 CAb were purchased from Proteintech Group, Inc. (Wuhan, China). CCN1 DAb and NHS-biotin were obtained from Abcam Trading Company Ltd. (Shanghai, China). *N*-(3-Dimethylamino-

DOI: 10.1021/acsami.9b12428
ACS Appl. Mater. Interfaces 2019, 11, 31427−31433

propyl)-*N*-ethylcarbodiimidehydrochloride (EDC) and *N*-hydroxysuccinimide (NHS) were received from J&K Scientific Ltd. (Beijing, China). Ruthenium(II) tris(4,4′-dicarboxylicacid-2,2′-bipyridyl) [Ru(dcbpy)$_3^{2+}$] was acquired from SunaTech, Inc. (Suzhou, China). All the DNA oligonucleotides were purchased by Shanghai Sangon Biological Engineering Technology & Services Co., Ltd. (Shanghai, China), and their nucleotide sequences were shown in Table 1. The

Table 1. DNA Sequences Employed in the Proposed Assay

Name	Sequences (5'-3')
Initiator I	HOOC-TAG CTT ATC AGA CTG ATG TTG A
Fc-H1	Fc-TGG AGT GTG ACA ATC GTG TTT GGG *CTT ATC AGA CTG ATG TTG ACG ATT GTC ACA CTC CAT CAA CAT CAG TC*
H2	*AGA CTG ATG TTG ATG GAG TGT GAC AAT CGT CAA CAT CAG TCT GAT AA*
ssDNA	GCC CAA ACA CGA TTG TCA CAC TTT TTT TTT TT-SH

human serum samples were obtained from Chongqing General Hospital (Chongqing, China). 0.1 M Na_2HPO_4, 0.1 M KH_2PO_4, and 0.1 M KCl were used for the preparation of phosphate buffer solution (PBS) (pH 7.4). TE buffer (pH 8.0) was prepared with 10 mM Tris-HCl and 1 mM ethylenediaminetetraacetic acid disodium salt (EDTA-2Na) solution with 12.5 mM $MgCl_2$. Double-distilled water was used throughout this study.

2.2. Instrumentation. A CHI 760E electrochemistry workstation (Shanghai Chenhua Instrument, Shanghai, China) was used to carry out cyclic voltammetric (CV), electrochemical impedance spectroscopy (EIS), and electrochemical deposition. A MPI-A ECL analyzer (Xi'an Remax Electronic Science & Technology Co. Ltd, Xi'an, China) was employed to monitor the ECL emissions with a conventional three-electrode system composed of a glassy carbon working electrode, a platinum wire counter electrode, and an Ag/AgCl (sat. KCl) reference electrode. The voltage of the photomultiplier tube (PMT) was proposed at 800 V and the range of continuous potential was from −0.5 to 1.5 V at a scanning rate of 100 mV s^{-1} in the process of ECL detection. The polyacrylamide gel electrophoresis was stained with Gen Green, and imaged in the Gel Doc XR+ system (Bio-Rad Laboratories Co. Ltd, CA, USA).

2.3. Fabrication of the Proposed ECL Biosensor. Firstly, the GCE (Φ = 3 mm) was polished to a mirror-liked surface by using 0.3 and 0.05 μm α-Al_2O_3 powder. And the polished electrodes were sonicated alternately in double distilled water and ethanol for 5 min to remove any adsorbed substances. Then, 3 μL of Nafion@Ru(dcbpy)$_3^{2+}$ (Nf@Ru) solution, which was prepared by dissolving Ru(dcbpy)$_3^{2+}$ in 5% Nafion, was dropped onto the surface of the cleaned GCE and the modified electrodes were kept at 37 °C for 3 h to acquire the Nf@Ru/GCE with a higher stable signal (Scheme 1B). Next, the Nf@Ru/GCE was electrodeposited in $HAuCl_4{\cdot}4H_2O$ solution (10 mg/mL, −0.2 V, 10 s) to achieve AuNPs platform. After that, 7 μL of 1 μM ssDNA was further coated on the surface of electrode and the proposed electrodes were incubated at 4 °C refrigerator overnight. Finally, 5 μL of 1 mM HT was used to block the electrode at 4 °C for 40 min to avoid nonspecific adsorption in the detection processes. Thus, the proposed biosensor HT/ssDNA/AuNPs/Nf@Ru/GCE was obtained for the detection reaction.

2.4. Preparation of CAb-Biotin and DAb-Initiator I. Specific antibodies are macromolecular proteins that contain free carboxyl groups and amino groups depending on their own chemical structure, which could be employed for the modification or labeling of various chemicals. The EDC/NHS system is a widely used bioconjugation strategy, which could activate the carboxyl group and catalyze the condensation reaction between the carboxyl group and amine group. NHS-biotin effectively reacting with the primary amine group ($-NH_2$) of proteins could be applied to label CCN1 CAb. With a similar reaction mechanism, the DAb-initiator I was assembled via the bioconjugation between the carboxyl group-modified initiator I and the amino groups on CCN1 DAb.

Conveniently, 10 mM NHS-biotin was prepared by dissolving 3.4 mg in 1 mL dimethyl sulfoxide and sitting for 10 min. Then, 10 μL of 10 mM NHS-biotin was mixed with 3 μL of CCN1 CAb (50 μg/150 μL) to obtain the CAb-biotin, which employed 0.5 mL PBS as buffer and reacted at 37 °C for 2 h. After that, the successfully assembled CAb-biotin was intercepted and purified through the ultrafiltration membrane. Finally, CAb-biotin was successfully acquired via redissolving in 1 mL PBS and stored in a 4 °C refrigerator for further use. CCN1 DAb was labeled by nucleotide initiator I through the EDC/NHS reaction. 100 μL of nucleotide initiator I (1 μM) was mixed with 100 μL of EDC (40 mM) accompanying continuous stirring for 2 h at 4 °C to promote the activation of the carboxyl group, which was modified on the 5 prime of initiator I. After the addition of 5 μL of DAb (200 μg/mL) and 100 μL of NHS (10 mM), the mixture was diluted with PBS to 1 mL and continually stirred at 4 °C overnight to obtain DAb-initiator I. Similar to the CAb-biotin purification process, DAb-initiator I also was reserved by the ultrafiltration membrane.

2.5. Combination of Sandwich Immunoassay and Strand Displacement Cycle. The manufacturing process of a dual antibody sandwich complex and CHA amplification is shown in Scheme 1A. First, the CAb-biotin was reacted with the streptavidin-magnetic beads through the specific reaction of the biotin−streptavidin system to obtain CAb-biotin/SA@MB. In addition, the CAb-biotin captured the target CCN1 of various concentrations via the special recognition between antigens and antibodies, causing the formation of CCN1/CAb-biotin/SA@MB. Afterward, the double antibody sandwich complex DAb-initiator I/CCN1/CAb-biotin/SA@MB was synthesized by the molecular interaction between CCN1 and DAb-initiator I. Eventually, the mixture solutions were incubated with 1 μM Fc-H1 and H2 at 37 °C for 90 min to promote the cycle amplification of the

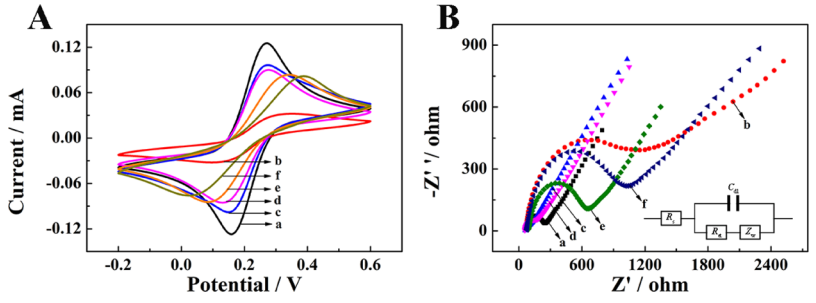

Figure 1. Characterization of biosensors with different modified stages based on CV (A) and EIS (B): (a) bare GCE, (b) Nf@Ru/GCE, (c) AuNPs/Nf@Ru/GCE, (d) ssDNA/AuNPs/Nf@Ru/GCE, (e) HT/ssDNA/AuNPs/Nf@Ru/GCE, and (f) Fc-H1−H2/HT/ssDNA/AuNPs/Nf@Ru/GCE. Inset, the equivalent circuit with model impedance data of EIS responses.

DOI: 10.1021/acsami.9b12428
ACS Appl. Mater. Interfaces 2019, 11, 31427−31433

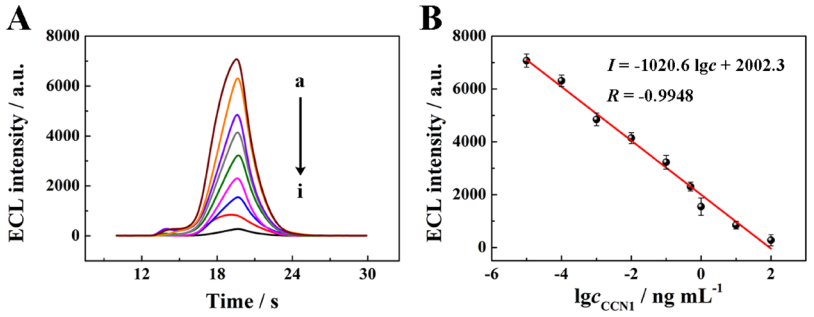

Figure 2. (A) Different concentrations of CCN1 were detected by the proposed ECL biosensor (a–i): 10 fg/mL, 100 fg/mL, 1 pg/mL, 10 pg/mL, 100 pg/mL, 500 pg/mL, 1 ng/mL, 10 ng/mL, and 100 ng/mL. (B) Calibration curve of the ECL response as a function of the concentration of CCN1. The potential scan was −0.5 to 1.5 V and the PTM was 800 V.

target-induced strand displacement reaction and the output Fc-H1–H2 duplex was obtained. The magnetic separation was conducted by the streptavidin-magnetic beads' strong attraction toward the magnetic shelf following every step of the whole manufacturing process to acquire the pure intermediates.

2.6. Measurement Procedure. The detailed ECL strategy of CCN1 detection was shown in Scheme 1B. Primarily, 7 μL of the output Fc-H1–H2 duplexes corresponding to different CCN1 concentrations were individually dropped onto the proposed biosensors HT/ssDNA/AuNPs/Nf@Ru/GCE with 90 min incubation time at 37 °C. After that, the obtained biosensors were immersed into 2 mL of 0.1 M PBS with TPrA (5 mM) as a co-reactant for ECL detection. The voltage of the PMT was set at 800 V with the potential range from −0.5 to 1.5 V.

3. RESULTS AND DISCUSSION

3.1. Electrochemical Behaviors of the Proposed ECL Biosensor. Both CV and EIS were effective methods for studying the electrode interface properties of the ECL biosensor. CV measurements were performed in 0.1 M PBS (pH 7.4) containing 5.0 mM $[Fe(CN)_6]^{3-/4-}$ ranged from −0.2 to 0.6 V with a scan rate of 100 mV s^{-1} for verifying the modification steps of the sensing interface. As we can see from Figure 1A, a pair of typical reversible redox peaks was observed on the bare GCE (curve a). After being modified with the Nf@Ru compound, the redox peak current sharply decreased (curve b) because of the Nf layer which hindered electron transfer. Then, the peak current obviously increased (curve c) because of the improved electron transfer and excellent conductivity of AuNPs which was electrodeposited onto the electrode surface. When ssDNA was successfully immobilized on the electrode, a decreased peak current was observed (curve d). The peak current was decreased continuously (curve e) after blocking with HT. Finally, when the target CCN1 (100 pg/mL) cycling-transformed output of Fc-H1–H2 was brought to the electrode surface through the hybridization reaction, a further decreased redox peak current was acquired (curve f).

At the same time, another useful electrochemical measurement, EIS was commonly utilized for characterizing the interface properties of the electrode to monitor the fabrication process (Figure 1B) based on the change of the electron transfer resistance (R_{et}), corresponding to the semicircle diameter at higher parts of the Nyquist plot. An initial R_{et} value about 163.7 Ω was acquired with the bare GCE (curve a). When the Nf@Ru compound was incubated onto the electrode surface, an obviously increased R_{et} about 1036.6 Ω was obtained (curve b). Then, AuNPs were electrodeposited on the electrode, a sharp decrease of R_{et} was observed (curve c, R_{et} = 35.7 Ω) owing to the excellent conductive property of AuNPs. The capture probe ssDNA was coated on the electrode via a Au–S bond, it could be seen that the R_{et} increased to about 98.2 Ω (curve d). In addition, when the modified electrode was incubated with HT, the R_{et} increased (curve e, R_{et} = 504.3 Ω) because HT blocked the interfacial electron transfer. When the Fc-H1–H2 DNA duplex was hybridized with ssDNA, the R_{et} increased to about 847.1 Ω (curve f). Based on the acquired results, it could be concluded that the ECL biosensor was successfully fabricated. Moreover, the modified equivalent circuit was shown in the inset of Figure 1B, in which R_s, C_{dl}, Z_w, and R_{et} presented the Ohmic resistance of the electrolyte, the double-layer capacitance, the Warburg-impedance, and the electron transfer resistance, respectively.

3.2. Analytical Performance of the ECL Biosensor. The detection process based on the immune response on the magnetic bead surface and the subsequent chain displacement reaction, successfully convert target CCN1 into specific DNA sequences. In addition, these converted DNA duplexes obtained by CHA were brought to the electrode surface for hybridizing with ssDNA, meanwhile, the signal-quenched molecule ferrocene was introduced for efficiently decreasing the ECL signal. The drop in ECL signals were directly related to the number of specific DNA sequences generated by the transformation, and further associated with the concentrations of the target protein CCN1. Owing to such an investigated relationship between signal intensities and target concentrations, the quantitative detection of CCN1 has been achieved.

To validate the performance of the ECL biosensor in CCN1 detection, the proposed biosensors were employed for the determination of CCN1 concentrations with 10 fg/mL, 100 fg/mL, 1 pg/mL, 10 pg/mL, 100 pg/mL, 500 pg/mL, 1 ng/mL, 10 ng/mL, and 100 ng/mL, respectively, and the corresponding data was shown in Figure 2A. The ECL intensity decreased with the increasing Fc-H1–H2 located on the electrode surface, which were associated with the concentrations of CCN1 in the range from 10 fg/mL to 100 ng/mL (Figure 2B). The linear equation of the proposed ECL signals was $I = -1020.6 \lg c + 2002.3$ with a correlation coefficient of −0.9948 and a detection limit of 3.9 fg/mL, which indicated that the proposed biosensor could be used for the quantitative detection of CCN1 with early cancer diagnosis and metastasis monitoring.

In contrast, the current conventional indirect immunofluorescence assay conducted for CCN1 detection is shown in Figure S2 in the Supporting Information. Furthermore, Table 2

DOI: 10.1021/acsami.9b12428
ACS Appl. Mater. Interfaces 2019, 11, 31427–31433

Table 2. Comparison of the Protein Detection with Some Different Analytical Strategies

method	target	detection limit	dynamic range	refs
electrochemical	MMP-2	30 fg/mL	100 fg/mL−20 ng/mL	28
photoelectrochemical	PSA	3 pg/mL	10 pg/mL−80 ng/mL	29
fluorescent	MUC1	230 fg/mL	1 pg/mL−20 ng/mL	30
ECL	CEA	16 fg/mL	100 fg/mL−100 ng/mL	31
ECL	AFP	400 fg/mL	1 pg/mL−1 μg/mL	32
ECL	CCN1	3.9 fg/mL	10 fg/mL−100 ng/mL	this study

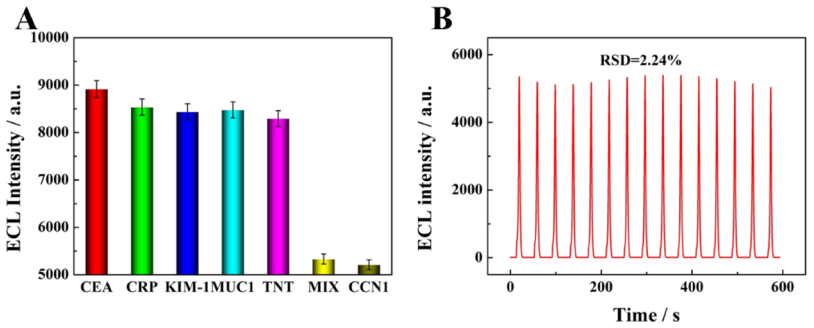

Figure 3. (A) Selectivity of the proposed ECL biosensor with different targets. (B) Stability of the proposed biosensor under consecutive cyclic potential scans for 15 cycles.

revealed the comparison of the performances of the designed ECL biosensor and some previously reported studies. Significantly, the working performance of the proposed biosensor for protein analysis was comparable and even superior to that of the previous ones.

3.3. Specificity and Stability of the ECL Biosensor. To investigate the specificity of the proposed ECL biosensor, the biosensor was examined with different interfering substances including 10 pg/mL carcinoembryonicantigen (CEA), hypersensitive C-reactive protein (hs-CRP), cardiac troponin T (cTnT), mucin 1 protein (Muc 1), and Kim-1. As shown in Figure 3A, there was a significant different ECL response between 1 pg/mL CCN1 and other interferences, indicating that the proposed ECL biosensor has achieved satisfactory specificity. Simultaneously, Figure 3B showed that the proposed ECL signals did not have obvious changes with 1 pg/mL CCN1 under consecutive cyclic potential scans for 15 cycles, and the relative standard deviations were 2.24%, illustrating the excellent stability of the ECL biosensor for detecting CCN1.

3.4. Analysis of the Biosensor in Human Serum Samples. For verifying the feasibility of the proposed CCN1 detection strategy, the ECL biosensors were implemented in the analysis of clinical serum samples, which were obtained from Chongqing General Hospital. In addition, the lab study results acquired by the proposed ECL immunoassay were compared with those obtained by the commercial ELISA applied in scientific research. As Table 3 indicated, these results obtained by two different assays have exhibited good coincidence with each other, demonstrating that the proposed ECL biosensor possessed well reliability and provided a promising tool in the clinical determination of CCN1.

4. CONCLUSIONS

In summary, a novel ECL biosensor was constructed based on sandwich immunoassay-induced target transformation assisted with CHA amplification for ultrasensitive detection of CCN1. Different from the normal immunoassay, the target CCN1 was first transformed to the oligonucleotide via a sandwich immunoassay, and the oligonucleotide triggered an efficient CHA amplification to produce massive hybrids containing a sticky end labeled with ferrocene, which could be immobilized on the $[Ru(dcbpy)_3^{2+}]$-modified electrode surface, performing a obviously quenched ECL signal related with the concentration of target CCN1. Significantly, by the integration of the immunoassay-induced target transformation and CHA amplification strategy, the proposed ECL biosensor performed the low detection limit, wide-linear range, and high selectivity. Most importantly, the proposed immunoassay could be easily and reasonably extended to electrochemical, chemiluminescent, and fluorescent assays for various protein targets, providing strong evidence for cancer diagnosis and monitoring recurrence.

Table 3. Results of CCN1 Detection in Human Serum Samples Using the Proposed ECL Assay and Commercial ELISA

samples	our method (pg/mL)	commercial method (pg/mL)	relative error (%)
1	8.3	9.4	−11.7
2	15.9	16.1	−1.2
3	21.3	24.7	−13.7
4	23.0	24.7	−6.8
5	218.1	211.1	3.3
6	633.6	668.7	−5.2

■ ASSOCIATED CONTENT

Supporting Information

The Supporting Information is available free of charge on the ACS Publications website at DOI: 10.1021/acsami.9b12428.

Performance of the CHA-mediated macromolecule conversion, optimization of experimental conditions, storage stability of the ECL assay, comparison of the proposed assay with other analytical strategies, comparison of the proposed ECL assay with or without CHA for protein and DNA detection, and the detection time

DOI: 10.1021/acsami.9b12428
ACS Appl. Mater. Interfaces 2019, 11, 31427−31433

of the proposed ECL assay compared with other studies (PDF)

AUTHOR INFORMATION

Corresponding Author

*E-mail: liaopu2015@163.com. Phone: +86-23-63519127. Fax: +86-23-63516241.

ORCID

Wen-Bin Liang: 0000-0002-9086-4974

Ruo Yuan: 0000-0003-3664-6236

Pu Liao: 0000-0002-9091-0758

Author Contributions

§H.-X.L. and C.-C.N. contributed equally to this work.

Notes

The authors declare no competing financial interest.

ACKNOWLEDGMENTS

This work was financially supported by the National Natural Science Foundation of China (81702075), Chongqing Natural Science Foundation (cstc2019jcyj-msxm1538) and the Fundamental Research Funds for the Central Universities (SWU118106), China.

REFERENCES

(1) Vrdoljak, E.; Bodoky, G.; Jassem, J.; Popescu, R. A.; Mardiak, J.; Pirker, R.; Čufer, T.; Bešlija, S.; Eniu, A.; Todorović, V.; Kubáčková, K.; Kurteva, G.; Tomašević, Z.; Sallaku, A.; Smichkoska, S.; Bajić, Ž.; Šikić, B. I. Cancer Control in Central and Eastern Europe: Current Situation and Recommendations for Improvement. *Oncologist* **2016**, *21*, 1183−1190.

(2) Chen, W.; Zheng, R.; Baade, P. D.; Zhang, S.; Zeng, H.; Bray, F.; Jemal, A.; Yu, X. Q.; He, J. Cancer Statistics in China, 2015. *CA-Cancer J. Clin.* **2016**, *66*, 115−132.

(3) Poleszczuk, J.; Luddy, K.; Chen, L.; Lee, J. K.; Harrison, L. B.; Czerniecki, B. J.; Soliman, H.; Enderling, H. Neoadjuvant radiotherapy of early-stage breast cancer and long-term disease-free survival. *Breast Cancer Res.* **2017**, *19*, 75.

(4) Alghulayqah, A.; Alghasab, N.; Amin, T.; Alkahtani, N.; Farhat, R.; Alzahrani, A. S. Long-term recurrence-free survival of adrenocortical cancer extending into the inferior vena cava and right atrium. *Medicine* **2017**, *96*, No. 18.

(5) McPhail, S.; Johnson, S.; Greenberg, D.; Peake, M.; Rous, B. Stage at diagnosis and early mortality from cancer in England. *Br. J. Cancer* **2015**, *112*, S108−S115.

(6) Armitage, E. G.; Barbas, C. Metabolomics in cancer biomarker discovery: Current trends and future perspectives. *J. Pharm. Biomed. Anal.* **2014**, *87*, 1−11.

(7) Li, W.; Li, C.; Zhou, T.; Liu, X.; Liu, X.; Liu, X.; Chen, D. Role of exosomal proteins in cancer diagnosis. *Mol. Cancer* **2017**, *16*, 145.

(8) Niu, C.-C.; Zhao, C.; Yang, Z.; Zhang, X.-L.; Pan, J.; Zhao, C.; Si, W.-K. Inhibiting CCN1 blocks AML cell growth by disrupting the MEK/ERK pathway. *Cancer Cell Int.* **2014**, *14*, 74.

(9) Sánchez-Bailón, M. P.; Calcabrini, A.; Mayoral-Varo, V.; Molinari, A.; Wagner, K. U.; Losada, J. P.; Ciordia, S.; Albar, J. P.; Martín-Pérez, J. Cyr61 as mediator of Src signaling in triple negative breast cancer cells. *Oncotarget* **2015**, *6*, 13520−13538.

(10) Jeong, D. J.; Heo, S.; Ahn, T. S.; Lee, S.; Park, S.; Kim, H.; Park, D.; Bae, S. B.; Lee, S. S.; Lee, M. S.; Kim, C. J.; Baek, M. J. Cyr61 Expression is associated with prognosis in patients with colorectal cancer. *BMC Cancer* **2014**, *14*, 164.

(11) Hou, C.-H.; Lin, F.-L.; Hou, S.-M.; Liu, J.-F. Cyr61 promotes epithelial-mesenchymal transition and tumor metastasis of osteosarcoma by Raf-1/MEK/ERK/Elk-1/TWIST-1 signaling pathway. *Mol. Cancer* **2014**, *13*, 236.

(12) Cheng, G.; Zhang, H.; Zhang, L.; Zhang, J. Cyr61 promotes growth of glioblastoma in vitro and in vivo. *Tumor Biol.* **2015**, *36*, 2869−2873.

(13) Wu, D. D.; Zhang, F.; Hao, F.; Chun, J.; Xu, X.; Cui, M.-Z. Matricellular Protein Cyr61 Bridges Lysophosphatidic Acid and Integrin Pathways Leading to Cell Migration. *J. Biol. Chem.* **2014**, *289*, 5774−5783.

(14) Jandova, J.; Beyer, T. E.; Meuillet, E. J.; Watts, G. S. The matrix protein CCN1/CYR61 is required for $\alpha_v\beta_5$-mediated cancer cell migration. *Cell Biochem. Funct.* **2012**, *30*, 687−695.

(15) Wei, J.; Yu, G. Z.; Shao, G. B.; Sun, A. Q.; Chen, M.; Yang, W. N.; Lin, Q. CYR61 (CCN1) is a metastatic biomarker of gastric cardia adenocarcinoma. *Oncotarget* **2016**, *7*, 31067−31078.

(16) Song, Y. F.; Xu, Z. B.; Zhu, X. J.; Tao, X.; Liu, J. L.; Gao, F. L.; Wu, C. L.; Song, B.; Lin, Q. Serum Cyr61 as a potential biomarker for diagnosis of colorectal cancer. *Clin. Transl. Oncol.* **2017**, *19*, 519−524.

(17) Zhang, Q.; Wu, J.; Cao, Q.; Xiao, L.; Wang, L.; He, D.; Ouyang, G.; Lin, J.; Shen, B.; Shi, Y.; Zhang, Y.; Li, D.; Li, N. A Critical Role of Cyr61 in Interleukin-17-Dependent Proliferation of Fibroblast-like Synoviocytes in Rheumatoid Arthritis. *Arthritis Rheum.* **2009**, *60*, 3602−3612.

(18) Liu, H.; Peng, F.; Liu, Z.; Jiang, F.; Li, L.; Gao, S.; Wang, G.; Song, J.; Ruan, E.; Shao, Z.; Fu, R. CYR61/CCN1 stimulates proliferation and differentiation of osteoblasts in vitro and contributes to bone remodelling in vivo in myeloma bone disease. *Int. J. Oncol.* **2017**, *50*, 631−639.

(19) Afsharan, H.; Navaeipour, F.; Khalilzadeh, B.; Tajalli, H.; Mollabashi, M.; Ahar, M. J.; Rashidi, M.-R. Highly sensitive electrochemiluminescence detection of p53 protein using functionalized Ru-silica nanoporous@gold nanocomposite. *Biosens. Bioelectron.* **2016**, *80*, 146−153.

(20) Rashidiani, J.; Kamali, M.; Sedighian, H.; Akbariqomi, M.; Mansouri, M.; Kooshki, H. Ultrahigh sensitive enhanced-electrochemiluminescence detection of cancer biomarkers using silica NPs/graphene oxide: A comparative study. *Biosens. Bioelectron.* **2018**, *102*, 226−233.

(21) Cheng, Z.; Choi, N.; Wang, R.; Lee, S.; Moon, K. C.; Yoon, S.-Y.; Chen, L.; Choo, J. Simultaneous Detection of Dual Prostate Specific Antigens Using Surface-Enhanced Raman Scattering-Based Immunoassay for Accurate Diagnosis of Prostate Cancer. *ACS Nano* **2017**, *11*, 4926−4933.

(22) Zhu, X.; Zhai, Q.; Gu, W.; Li, J.; Wang, E. High-Sensitivity Electrochemiluminescence Probe with Molybdenum Carbides as Nanocarriers for α-Fetoprotein Sensing. *Anal. Chem.* **2017**, *89*, 12108−12114.

(23) Yang, H.; Wang, H.; Xiong, C.; Chai, Y.; Yuan, R. Highly sensitive electrochemiluminescence immunosensor based on ABEI/H_2O_2 system with PFO dots as enhancer for detection of kidney injury molecule-1. *Biosens. Bioelectron.* **2018**, *116*, 16−22.

(24) Li, B.; Jiang, Y.; Chen, X.; Ellington, A. D. Probing Spatial Organization of DNA Strands using Enzyme-free Hairpin Assembly Circuits. *J. Am. Chem. Soc.* **2012**, *134*, 13918−13921.

(25) Mudiyanselage, A. P. K. K. K.; Yu, Q.; Leon-Duque, M. A.; Zhao, B.; Wu, R.; You, M. Genetically Encoded Catalytic Hairpin Assembly for Sensitive RNA Imaging in Live Cells. *J. Am. Chem. Soc.* **2018**, *140*, 8739−8745.

(26) Chen, X.; Briggs, N.; McLain, J. R.; Ellington, A. D. Stacking nonenzymatic circuits for high signal gain. *Proc. Natl. Acad. Sci. U.S.A.* **2013**, *110*, 5386−5391.

(27) Tang, Y.; Lin, Y.; Yang, X.; Wang, Z.; Le, X. C.; Li, F. Universal strategy to engineer catalytic DNA hairpin assemblies for protein analysis. *Anal. Chem.* **2015**, *87*, 8063−8066.

(28) Kou, B.-B.; Chai, Y.-Q.; Yuan, Y.-L.; Yuan, R. PtNPs as Scaffolds to Regulate Interenzyme Distance for Construction of Efficient Enzyme Cascade Amplification for Ultrasensitive Electrochemical Detection of MMP-2. *Anal. Chem.* **2017**, *89*, 9383−9387.

(29) Shu, J.; Qiu, Z.; Zhou, Q.; Lin, Y.; Lu, M.; Tang, D. Enzymatic Oxydate-Triggered Self-Illuminated Photoelectrochemical Sensing

DOI: 10.1021/acsami.9b12428
ACS Appl. Mater. Interfaces 2019, 11, 31427−31433

Platform for Portable Immunoassay Using Digital Multimeter. *Anal. Chem.* **2016**, *88*, 2958−2966.
(30) Yang, W.; Shen, Y.; Zhang, D.; Xu, W. Protein-responsive rolling circle amplification as a tandem template to drive amplified transduction of fluorescence signal probes for highly sensitive immunoassay. *Chem. Commun.* **2018**, *54*, 10195−10198.
(31) Zhou, Y.; Chen, S.; Luo, X.; Chai, Y.; Yuan, R. Ternary Electrochemiluminescence Nanostructure of Au Nanoclusters as a Highly Efficient Signal Label for Ultrasensitive Detection of Cancer Biomarkers. *Anal. Chem.* **2018**, *90*, 10024−10030.
(32) Mo, G.; He, X.; Zhou, C.; Ya, D.; Feng, J.; Yu, C.; Deng, B. A novel ECL sensor based on a boronate affinity molecular imprinting technique and functionalized SiO_2@CQDs/AuNPs/MPBA nanocomposites for sensitive determination of alpha-fetoprotein. *Biosens. Bioelectron.* **2019**, *126*, 558−564.

DOI: 10.1021/acsami.9b12428
ACS Appl. Mater. Interfaces 2019, 11, 31427−31433